Temperature, Pressure, and Heat Transfer near Condensing Bubbles

DIETER NORDMANN and FRANZ MAYINGER
Institut für Verfahrenstechnik
Technische Universität Hannover, West Germany

ABSTRACT

For a better understanding of the physical phenomena involved in subcooled boiling the growth and especially the collapse of bubbles at free convection in water was investigated experimentally. In order to eliminate the influence of the inhomogeneous temperature field at a heated wall the investigations were carried out injecting single vapor bubbles by a nozzle. As measuring techniques highspeed cinematography and holographic interferometry were used. Additionally the temporal pressure behaviour in the environment of the growing and collapsing bubbles was measured by sensitive pressure probes. The experiments were performed for a range of pressures from 0.5 to 4 bar and for subcoolings from 3 to 80 K.

NOMENCLATURE

Capital Letters

N'	molar refractivity	m^3/mol
R	universal gas constant in equation (1)	8.3143 J/molK
R	bubble radius	m
S'	interference order	
T	temperature	K
ΔT	subcooling T_v-T_l	K

Lower Case Letters

c	specific heat capacity	J/kgK
Δh_v	specific latent heat of vaporization	J/kg
k	wave length of the laser light	m
l	model length	m
n	refractive index	-

p	pressure	N/m^2
r	ordinate	m
t	time	s
u	velocity	m/s

Greek Letters

α	heat transfer coefficient	W/m^2K
Δ	difference	
λ	thermal conductivity	W/mK
ν	kinematic viscosity	m^2/s
ρ	mass density	kg/m^3

Subscripts

c	collapse
l	liquid
v	vapor
w	wall

Dimensionless Numbers

$$Ja = \frac{c_l \cdot \rho_l \cdot \Delta T}{\rho_v \cdot \Delta h_v}$$

$$Re = \frac{2 \cdot R \cdot u}{\nu}$$

INTRODUCTION

The thermo- and hydrodynamic phenomena during the collapse of vapor bubbles in subcooled liquids are of scientific interest for the better understanding of the instability condition in two-phase flows. They are also of great significance for the practical layout of heat generating systems with high power densities, e.g. oil-fired boilers, chemical reactors and especially the core of water cooled nuclear reactors.

In the literature the growth and collapse of bubbles is described by the laws of heat transfer or liquid-inertia depending on the liquid subcooling. It is the aim of our investigations to determine the thermo- and hydrodynamic conditions, whether the condensation is controlled by inertia or heat transfer effects. The investigated pressure range varies from 0.5 to 4 bar and subcoolings between 3 and 80 K were used. As measuring techniques the holographic interferometry and the high speed cinematography are used. The interferometry allows to observe the temperature field in the boundary layer around the bubble and thus allows to determine the heat transfer at the phase boundary. The cinematography gives information on the decrease of the bubble volume.

Inertia effects are indicated by signals of sensitive pressure probes, which are positioned near the collapsing bubble.

In order to obtain a clear and usuable result it is necessary to reduce the investigated range of parameters. To eliminate the influence of the inhomogeneous temperature field at a heated wall the investigations were carried out injecting single vapor bubbles by a nozzle. By use of a vertical countercurrent flow at a low velocity a homogeneous temperature field could be established in the test chamber.

MEASURING TECHNIQUES

The left part of Fig. 1 schematically shows the test chamber with the nozzle holder for the injection of saturated vapor into

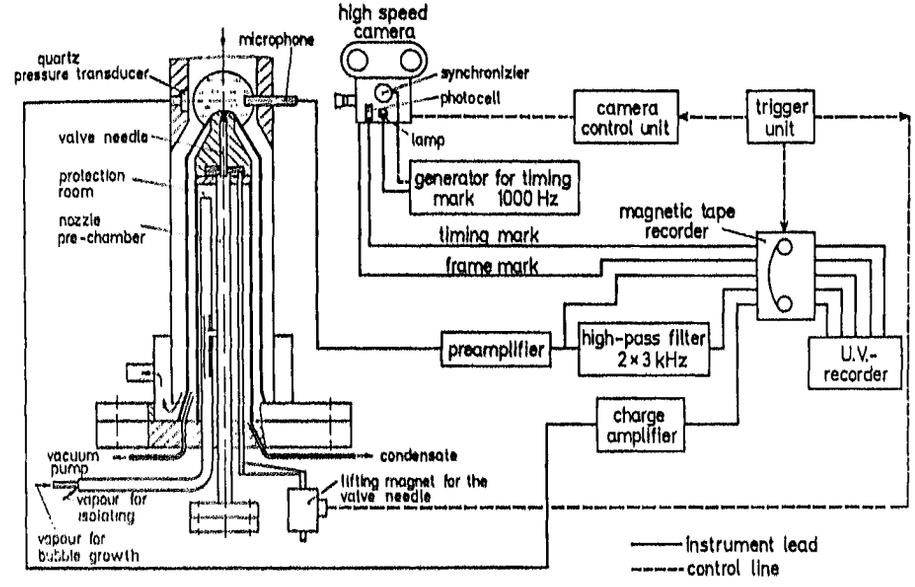

Fig. 1 Testsection with measuring equipment for recording the pressure oscillations

the subcooled liquid. The chamber is built in a water loop to maintain the operating conditions. The vapor flows into the nozzle holder through two coaxially arranged tubes. The vapor needed for the bubbles growth flows in the inner tube and the vapor insulating the nozzle holder in the annulus. By this construction the prechamber of the nozzle is guard-heated by the insulating vapor. To get an additional insulation against the circulating subcooled liquid, the shell of the nozzle holder was performed by a double wall construction, the gap could be evaluated if necessary. Doing holographic interferometry it is important, to film

the first bubbles growing at the nozzle end, because only these ones are surrounded by an undisturbed temperature field. Therefore the nozzle must not be opened before the highspeed camera is started.

In order to registrate the bubble emanated pressure waves on the magnetic tape, two sensitive pressure probes are installed rectangular to the windows of the test chamber at the height of the nozzle end. From the pressure oscillograms we can obtain some information about the influence of inertia forces. The signals were recorded simultaneously with the highspeed film. The measuring equipment used is shown on the right hand side of the figure 1. The signal of the microphone was recorded twice, firstly the original one and secondly the highpass filtered ($f > 3$ kHz) one. This is necessary to identify high frequency pulses, appearing at the end of the collapse period. The highspeed camera and the opening of the nozzle valve are triggered by the magnetic tape recorder, when the end-velocity is come up to 60 inch/s. To compare the record of the magtape to each frame of the highspeed film, the first 1.000 Hz timing mark was used. The timing mark generator was set to work after five meters film length. With help of a photocell each timing mark and a signal of each frame were recorded on the tape.

As already mentioned in the introduction the temperature field at the interphase of the bubbles was investigated with the holographic interferometry. The principle of this measuring technique shall not be explained in this paper (See ref. /1,2,3,4/.). To perform measurements at bubbles a special holographic technique, the so called real-time-method was used. A very often applied arrangement of the required optical setup is shown in Fig. 2. By means of a beam splitter the laser beam is divided into an object and reference beam. Both beams are then expanded to parallel waves by a telescope. The object wave passes through the test section, in which the temperature field is to be examined, whereas the reference wave falls onto the photographic plate, the so called hologram. After the first exposure by which the comparison wave is recorded, the hologram is developed and fixed. Remaining at its place and repositioned accurately, the comparison wave is reconstructed continuously by illuminating the hologram with the reference wave. The reconstructed wave can now be superposed onto the momentary object wave. If the object wave is not changed and the hologram precisely repositioned, no interference fringes will be seen at first (infinite-fringe-field adjustment). Now the heat transfer process, which is to be examined, can be started. In our example the wave receives an additional phase shift passing through the temperature field of a growing bubble. Behind the hologram both waves interfere with each other, and the changes of the interference pattern can be continuously observed or photographed on still or movie film up to 8.000 frames per second.

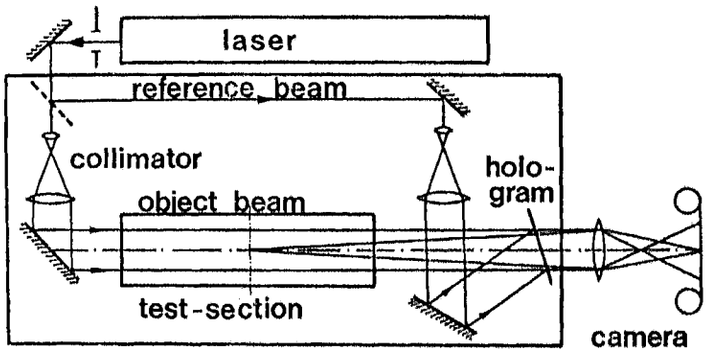

Fig. 2 Optical arrangement of a holographic interferometer

From the recorded interference pictures the phase shifting of the second wave against the first one can be obtained and the temperature behaviour can be calculated from this information. If the fluid is a gas, one can use the following formula:

$$T(x,y) = \left[\frac{S'(x,y)\cdot 2\cdot R\cdot k}{3\cdot N'\cdot p\cdot l} + \frac{1}{T_\infty}\right]^{-1} \qquad (1)$$

To assign each interference line to a temperature level the comparison value T_∞ has to be measured at one point by a conventional method, e.g. with thermocouples. With respect to liquids in the most practical cases the following simple equation can be used:

$$\Delta T' = \frac{S'(x,y)\cdot k}{l}\,\frac{1}{dn/dT} \qquad (2)$$

with the constant for water

$$\frac{dn}{dT} \approx 10^{-4}\left[\frac{1}{K}\right]$$

Often local heat transfer coefficients are of special interest. In this case the temperature gradient at the wall is determined, and assuming a laminar boundary layer near by the wall, the heat transfer coefficient is obtained by:

$$\alpha = \frac{-\lambda\cdot(dT/dy)_w}{T_w - T_\infty} \qquad (3)$$

The interferometry offers two possibilities to indicate the change of the refractive index distribution resulting from a temperature gradient: In a field without fringes by the appearing interference fringes and in a given fringe field by its deformation. At first both methods were applied separately in order to determine the temperature gradient at the interphase of the bubbles. Using an infinite fringe field the interference fringes could not be evaluated due to the very thin thermal boundary layer. Thus the determination of the temperature gradient was not possible. The fluiddynamic processes, however, as for example the drift flow,

could be observed. With a given fringe field, however, it was possible to obtain deformations of the fringes. The slope could be used for the calculation of the temperature gradient. For the simultaneous application of both methods the optical arrangement as shown in Fig. 3 was developed. In this arrangement two reference

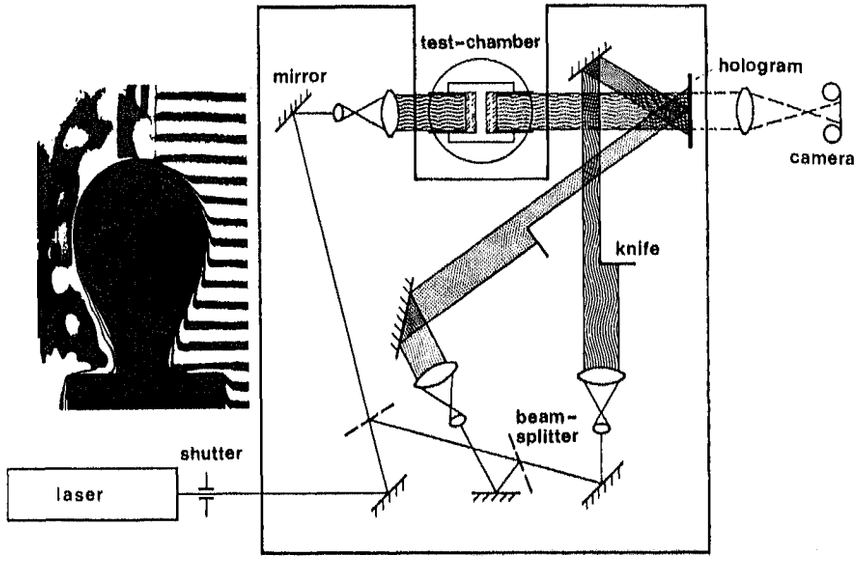

Fig. 3 Holographic interferometer with two reference beams for the investigation of single objects

beams are required. Only one half of each beam is used to illuminate the hologram plate. In addition it is possible to give two different fringe fields by the shown set-up. In the case of a temperature gradient the fringes of one field are deflected to the upper side of the picture, whereas the fringes of the other field are deflected to the lower part of the interference picture (see Fig. 4). This combination was very successful in determining the local temperature gradient at a growing bubble as shall be shown later.

Fig. 4 Interference picture of a bubble with fringe deflection in two directions

EXPERIMENTAL RESULTS

Fig. 5 shows a typical pressure oscillogram for low subcoolings in the upper part and for a subcooling of 83 K in the lower part of the figure. Comparing the oscillograms one has to consider the different time scale. At the high subcooling the bubble collapse within 4 ms, whereas at low subcooling the collapse time is 33 ms. The moment of detachment coincides with a pressure minimum, which is in agreement with the results of Kemnade /5/ obtained with gas bubbles. The maximum pressure peak is at low subcooling 11 mbar, at high subcooling 20 mbar. The high frequent pressure oscillations occuring after detachment probably result from waves at the bubble surface. Especially at high subcoolings surface waves could be observed by aid of the highspeed films.

At low subcoolings up to 20 K no pressure peaks of high frequency could be observed during the condensation period for the so far investigated pressure range of 1 - 4 bar. At higher subcoolings pressure peaks occur sporadically at the end of the collapse period, as can be seen especially when regarding the filtered signals. The appearance of pressure pulses indicates that inertia forces are effective.

A dependence of the maximum amplitude of the pressure oscillations at the end of the condensation on the subcooling could not be found. During detachment, however, the peak is a function of subcooling and system pressure. Therefore it seemed useful to plot the pressure peaks during detachment versus the Jakob-number, as is shown in Fig. 6. The Ja-number was calculated with the sub-

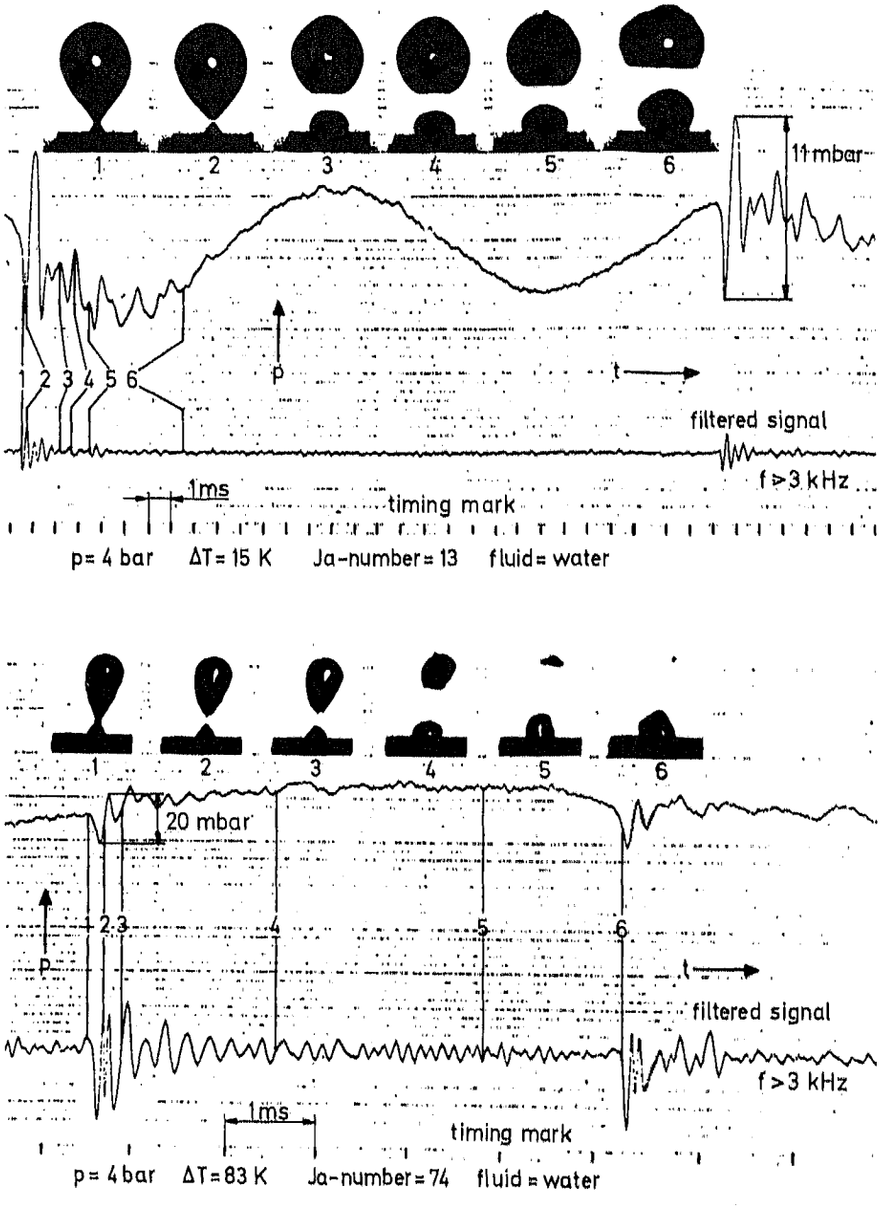

Fig. 5 Comparison of pressure oscillograms registrated in the surrounding of condensing vapor bubbles at low subcooling (upper curves) and high subcooling (lower curves)

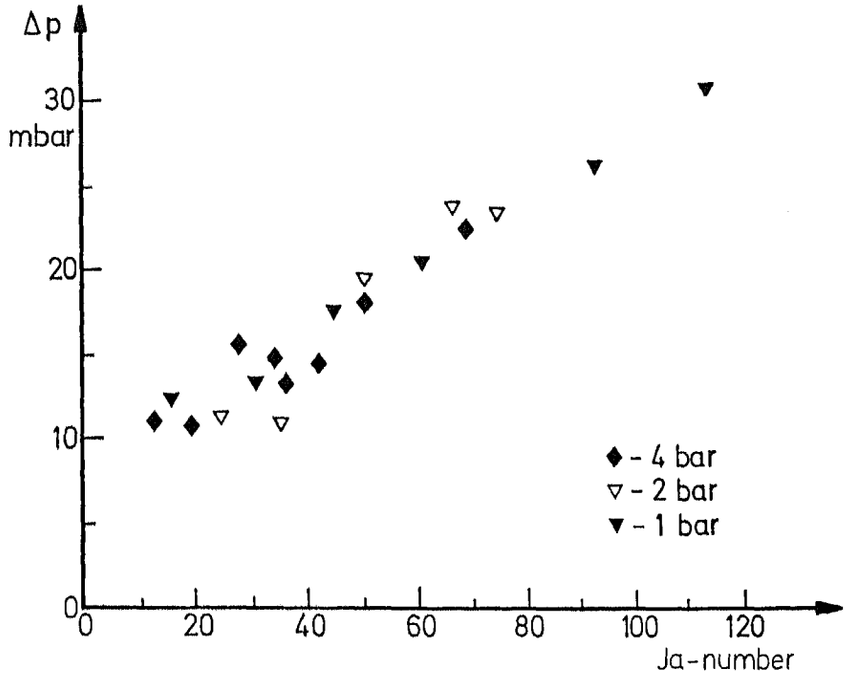

Fig. 6 Maximum pressure peaks at the moment of detachment of steam bubbles

cooling. The frequencies occuring at detachment and during collapse are shown in Fig. 7. The measured values cannot be predicted with equations for the eigenfrequency of bubbles which are known from the literature.

From the highspeed film one obtain information about the volume-decrease of the bubbles. The collapse-time can be plotted versus the Ja-number as is shown in Fig. 8. The experimental data can be well fitted by a simple equation:

$$t_c = 5{,}1 \cdot Ja^{-1{,}75} \qquad (4)$$

The next figures show some example of our results which were obtained by aid of the holographic interferometry: The differences during the collapse of bubbles at low and high subcooling shall be discussed by the example of two picture sequences (Fig. 9). On the right hand side of the pictures a horizontal fringe pattern is given. A temperature gradient causes a deflection of the fringes, whereas on the left hand side an infinite fringe field was adjusted as already explained before. The upper picture sequence shows the phenomena in the surrounding of a bubble in water at a

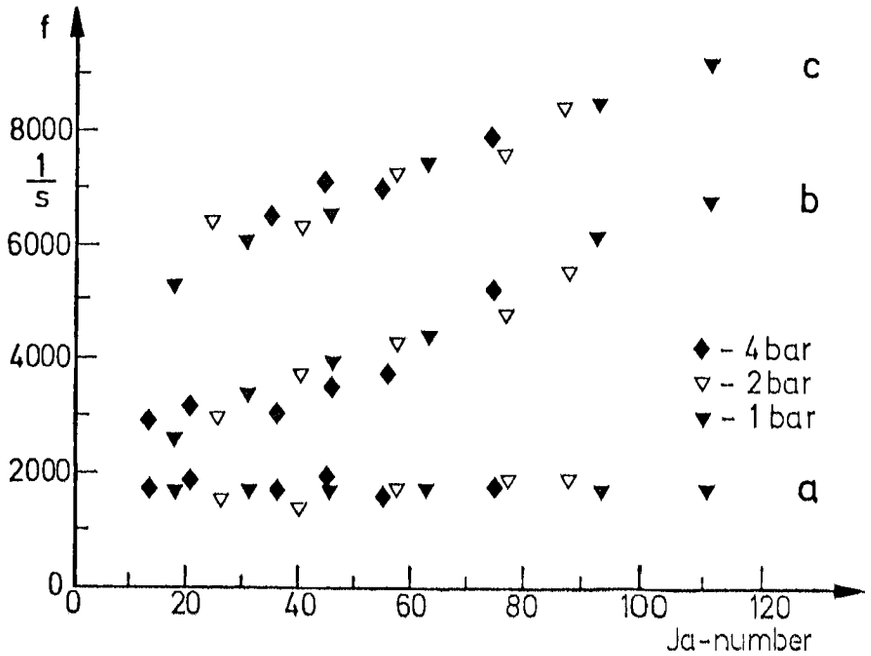

Fig. 7 Frequencies of pressure peaks: a) after detachment
b) after detachment (filtered signal)
c) to the end of the collapse period (filtered signal)

subcooling of 3 K. The vapor bubble detaches and rises. The rising period is superimposed by the collapse. In this example the Reynolds-number formed with the rising velocity is 3500 a short time after detachment. At high subcoolings as is shown in the lower picture sequence the position of the bubble center only changes insignificantly. The collapse takes place at the nozzle end.

At low subcoolings a thin boundary layer develops at the interphase as a result of the condensation, which starts when the head of the bubble comes out of the nozzle. In this layer the heat transfer takes place by conduction. During the growth period and a short period after the detachment this layer surrounds nearly the whole surface of the bubble and thereby stabilizes the interphase. In the region of the bubble foot the surface is submitted to strong changes resulting from the contraction and the drift flow. Sometimes flow eddies can be observed below the rising bubbles.

At high subcoolings the phase boundary at the bubble head is full of fissures as a result of strong dynamic local flow processes increasing the heat transfer. In contrary to the processes at low subcooling first at all a lateral decrease of the bubble vo-

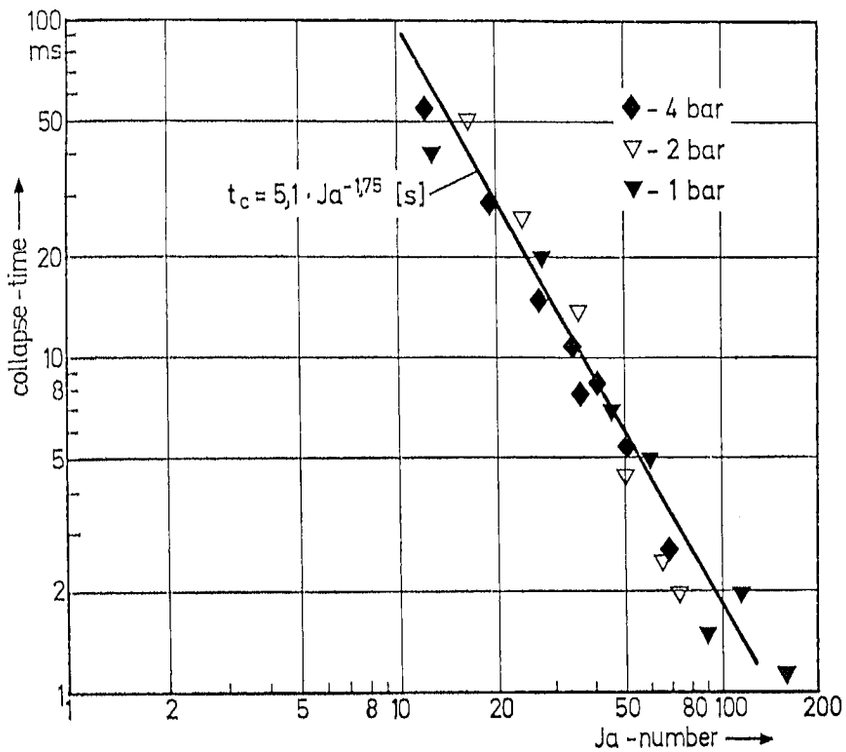

Fig. 8 Collapse-time versus Jakob-number

lume can be observed, which indicates inertia effects. The boundary layer is very turbulent and the bubble collapses quickly. At low subcooling the stabilizing thin boundary layer stays at the bubble head during the first period of the bubble life and the condensation mainly occurs at the bubble foot due to the drift flow. In the presented examples the collapse-time is 70 ms at the low subcooling and 6 ms at the high subcooling.

The temperature gradient at the phase boundary was calculated with help of the Abel-correction analogous to a cylindrical refractive index distribution as was already presented by Hauf and Grigull /3/. It is based on the assumption, that the light beam is not deflected by the boundary layer. From the interference picture shown on the right hand side of Fig. 10 the deflection of given horizontal and vertical fringe fields was evaluated. The determined temperature differences refer to the undisturbed surrounding fluid. The temperature gradient is higher at the head of the bubble than at its side. Resulting from the flow at the stag-

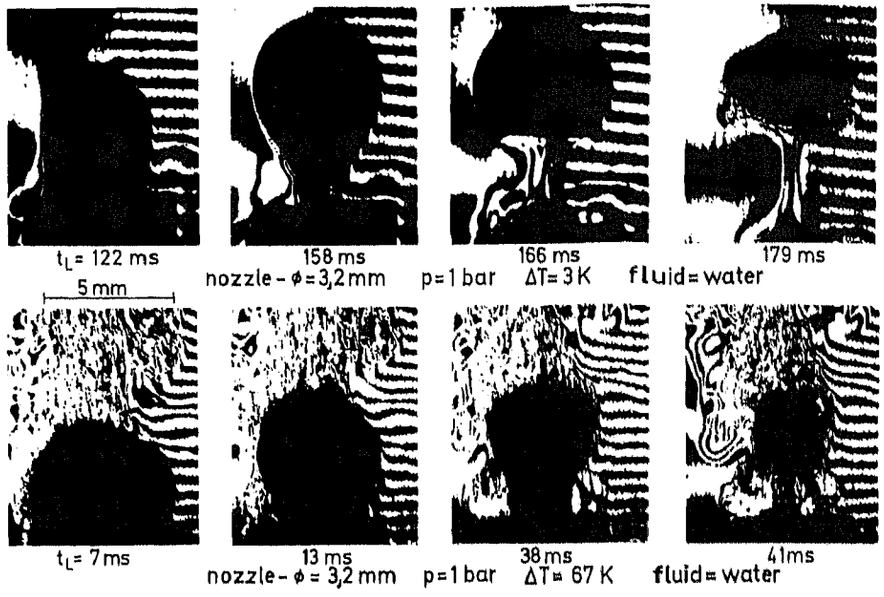

Fig. 9 Interference pictures of growing and collapsing steam bubbles at a subcooling of 3 K (upper sequence), respectively at a subcooling of 67 K (lower sequence). Left hand sides of the pictures without fringes, right hand side with interference pattern.

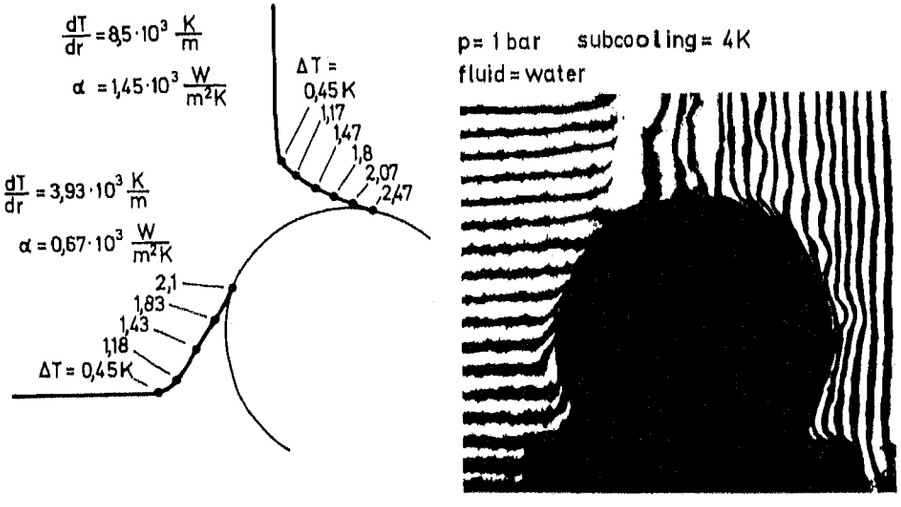

Fig. 10 Calculated temperature gradients and heat transfer coefficients at the head and the side of a steam bubble

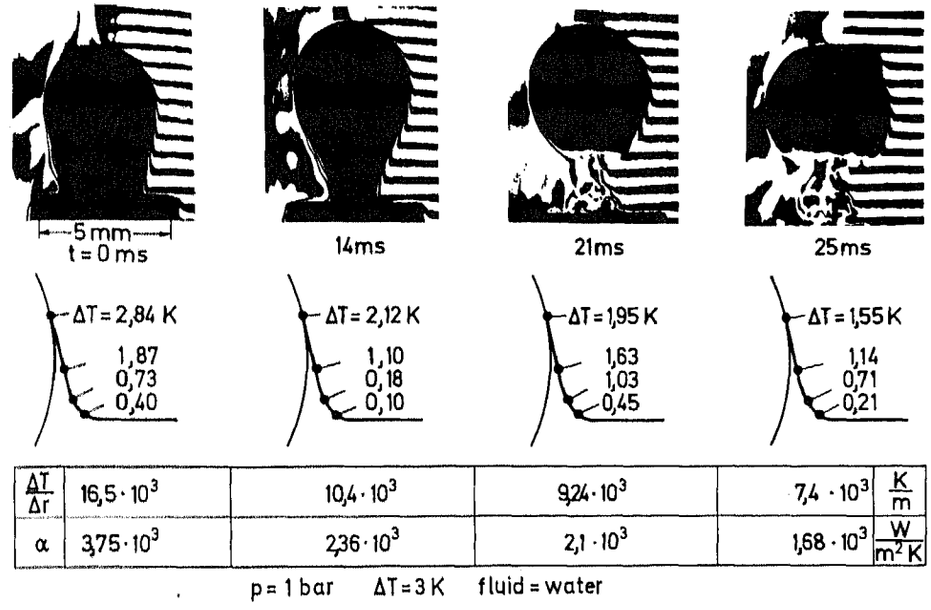

$\frac{\Delta T}{\Delta r}$	$16,5 \cdot 10^3$	$10,4 \cdot 10^3$	$9,24 \cdot 10^3$	$7,4 \cdot 10^3$	$\frac{K}{m}$
α	$3,75 \cdot 10^3$	$2,36 \cdot 10^3$	$2,1 \cdot 10^3$	$1,68 \cdot 10^3$	$\frac{W}{m^2K}$

p = 1 bar ΔT = 3 K fluid = water

Fig. 11 Temperature gradients and heat transfer coefficients during detachment of a steam bubble

nation point, which is induced by the growing bubble the boundary layer at the head is thinner. With the assumption of a laminar boundary layer at the interphase the local heat transfer coefficient was calculated from the temperature gradient, as was already stated in equation (3).

Fig. 11 shows the calculated results before and after detachment of a bubble. The boundary layer grows due to the instationary heat conduction and decreasing bubble radius. The heat transfer coefficients were determined between $0.6 \cdot 10^3$ and $3.75 \cdot 10^3$ W/m²K in the experiments done till now. In the literature values are reported between $0.5 \cdot 10^3$ and 10^4 W/m²K, which were calculated by the volume decrease of the bubbles.

CONCLUSIONS

By the investigations with the holographic interferometry it was possible to get a better knowledge of the heat and mass transfer processes during bubble collapse. At low subcooling the local heat transfer coefficient could be calculated from the interference pictures. By a comparison of the pressure oscillograms with the highspeed films it was stated, that the influence of inertia effects gains importance above a subcooling of 20 K. The greatest

pressure peaks occur at the moment of detachment with bubbles produced at nozzles.

The informations obtained from the performed experiments shall be the basis of an analytical description of the bubble condensation process.

REFERENCES

1. Mayinger, F., and Panknin, W. 1976. Holography in Heat and Mass Transfer. 5th Int. Heat Transfer Conference, VI, 28 Tokio.

2. Panknin, W. 1977. Eine holographische Zweiwellenlängen-Interferometrie zur Messung überlagerter Temperatur- und Konzentrationsgrenzschichten. Diss. T.U. Hannover.

3. Hauf, W., and Grigull, U. 1970. Optical Methods in Heat Transfer. Advances in Heat Transfer. Academic Press, New York. Vol. 6: 133 - 366.

4. Nordmann, D. 1976. Interferometric Investigations of Bubble Growth and Collapse in Subcooled Liquids. Proceedings of the NATO Advanced Study Institute on Two-Phase Flows and Heat Transfer. Aug. 16 - 27, Istanbul.

5. Kemnade, J. 1977. Blasenbildung und Phasengrenzfläche beim Dispergieren von Gasen in Flüssigkeiten an einzelnen Gaszulauföffnungen. Diss. TH Karlsruhe.